ISSN 0018-151X, High Temperature, 2018, Vol. 56, No. 2, pp. 201–207. © Pleiades Publishing, Ltd., 2018.
Original Russian Text © R.M. Khusnutdinoff, A.V. Mokshin, A.L. Bel'tyukov, N.V. Olyanina, 2018, published in Teplofizika Vysokikh Temperatur, 2018, Vol. 56, No. 2, pp. 211–218.

THERMOPHYSICAL PROPERTIES OF MATERIALS

Viscosity of Cobalt Melt: Experiment, Simulation, and Theory

R. M. Khusnutdinoff[a], *, A. V. Mokshin[a], **, A. L. Bel'tyukov[b], and N. V. Olyanina[b]

[a] *Kazan Federal University, Kazan, Russia*
[b] *Physical-Technical Institute, Ural Branch of the Russia Academy of Sciences, Izhevsk, Russia*
**e-mail: khrm@mail.ru*
***e-mail: anatolii.mokshin@mail.ru*

Received December 23, 2016

Abstract—The results of experimental measurements, molecular dynamics simulation, and theoretical calculations of the viscosity of a cobalt melt in a temperature range of 1400–2000 K at a pressure $p = 1.5$ bar corresponding to an overcooled melt at temperatures of 1400–1768 K and an equilibrium melt with temperatures from the range 1768–2000 K are presented. Theoretical expressions for the spectral density of the time-dependent correlation function of the stress tensor $\tilde{S}(\omega)$ and kinematic viscosity ν determined from the frequency and thermodynamic parameters of the system are obtained. The temperature dependences of the kinematic viscosity for the cobalt melt are determined experimentally by the torsional oscillation method; numerically, based on molecular simulation data with the EAM potential via subsequent analysis of the time correlation functions of the transverse current in the framework of generalized hydrodynamics; and by the integral Kubo–Green relation; they were also determined theoretically with the Zwanzig–Mori memory functions formalism using a self-consistent approach. Good agreement was found between the results of theoretical calculations for the temperature dependence of the kinematic viscosity of the cobalt melt using experimental data and the molecular dynamics simulation results. From an analysis of the temperature dependence of the viscosity, we obtain an activation energy of $E = (5.38 \pm 0.02) \times 10^{-20}$ J.

DOI: 10.1134/S0018151X18020128

INTRODUCTION

Amorphous-forming fluids that do not crystallize upon cooling and retain a disordered structure down to very low temperatures are a subject of intensive research in condensed matter physics [1–4]. A specific feature of such systems is associated with the temperature dependence of the viscosity (or the structural relaxation time), which varies by more than 15 orders of magnitude when passing from the liquid to the amorphous phase [5]. Amorphous metallic alloys (AMAs) are of particular interest, since they have unique physicomechanical properties [6–10]. Typically, AMAs are a multicomponent system with a high glass-forming ability that forms an amorphous phase at cooling with the rates $\gamma = (10^4–10^7)$ K/s [11, 12]. As shown in numerous molecular dynamics studies [13–19], an amorphous phase can also be obtained in the case of one-component (pure) metals as a result of superfast quenching ($\gamma = 10^{11}–10^{13}$ K/s). It is noteworthy that ferromagnetic transition metals (Fe, Ni, and Co), which are widely used in the aerospace industry, represent a particular case of single-component glass-forming metallic systems [7, 8, 20]. In this case, cobalt, as compared with iron and nickel, remains poorly understood. Thus, in particular, problems related to transport processes (self-diffusion, viscosity, thermal conductivity, and electrical conductivity) and the mechanisms by which collective excitations propagate in an equilibrium liquid and supercooled cobalt phases are unclear. This is partially due to the lack of experimental viscosimetry, inelastic X-ray, and neutron scattering data for this substance [20, 21]. The known experimental data on the viscosity of equilibrium liquid cobalt obtained by different researchers [22] reveal a significant (above 30%) discrepancy, which indicates the need for further research to clarify the absolute values of viscosity. Note that no viscosity values of the supercooled cobalt melt are currently found in the scientific literature.

This paper discusses the results of experimental measurements and molecular dynamics calculations of the viscosity of a cobalt melt in equilibrium liquid and supercooled phases. The kinematic viscosity was determined for the domain above and below the melting point $T_m(\mathrm{Co}) = 1768$ K: in the experiment for the temperature range $T = 1506–1969$ K and in simulation for 1400–2000 K.

EXPERIMENTAL

Experimental measurements were carried out for cobalt metal grade K0, which has a weight fraction of cobalt of at least 99.98% and contains the following impurities: 0.003% of Fe; less than 0.005% of Ni and C;

0.001% of Si, Cu, Mg, Zn, and Al; and <0.001% of O. The kinematic viscosity ν was measured by the method of torsional vibrations of a cylindrical crucible with a melt in the Shvidkovskii variant [23] with an automated set-up [24] in a protective helium atmosphere. Cylindrical Al_2O_3 cups with an internal diameter of ~17 mm and a height of ~42 mm were used as crucibles. To prevent the uncontrolled influence of the oxide film that is formed on the surface of the alloy during the measurement process, an Al_2O_3 lid was placed over the sample in the crucible. The lid construction is described in [25]. The gap between the side walls of the crucible and the lid was 0.2–0.3 mm. During the measurements, the lid tightly adhered to the upper boundary of the melt, providing a reliable friction surface. Rotation of the lid relative to the crucible was not possible.

The temperature dependences of the viscosity were measured in a heating regime from the melting point of cobalt to 1973 K and subsequent cooling to its crystallization in steps of 15–25 K. At each temperature, the melt was held for 20 min, after which no less than ten measurements were performed. The temperature of the melt was determined with an accuracy of ±5 K with a tungsten-rhenium thermocouple, 3–4 mm under the bottom of the crucible, calibrated for the melting points of pure metals (Al, Cu, Ni, Fe).

The kinematic viscosity values were calculated by numerical solving the equation of motion of the cup [23, 24]:

$$\mathrm{Re}(L) + \frac{\delta}{2\pi}\mathrm{Im}(L) - 2I\left(\frac{\delta}{\tau} - \frac{\delta_0}{\tau_0}\right) = 0,$$

where I is the moment of inertia of the suspension system; δ, τ, δ_0, τ_0 are the damping decrement and the period of oscillations of the suspension system with and without a melt, respectively; $\mathrm{Re}(L)$ and $\mathrm{Im}(L)$ and the real and imaginary parts of the friction function, taking into account two side surfaces of friction.

The thermal expansion of the crucible material entered the value of the sample radius R, taking into account that, in the range from 273 K to 2073 K, the mean linear thermal expansion coefficient of Al_2O_3 is 9.0×10^{-6} deg^{-1} [26]. The height of the melt in the crucible was calculated by the equation

$$H = \frac{m}{\pi R^2 \rho},$$

where m is the sample weight and ρ is the density of the cobalt melt, kg/m^3. The density of liquid cobalt was calculated by the equation obtained [22] by averaging the data from various authors:

$$\rho = 6172.152 - 0.936T.$$

To estimate the errors in measuring viscosity, the method described in [27], was used. It was established that the relative error of the obtained kinematic viscosity values does not exceed 4%, with an error in a single experiment of 2%.

SIMULATION

The molecular dynamics simulations of the cobalt melt were perfomed in an isothermally isobaric (NpT) ensemble in a temperature range of 1400–2000 K and at $p = 1.5$ bar. The system consisted of $N = 4000$ atoms in a cubic cell with periodic boundary conditions. The interaction between atoms was taken into account by the EAM potential [28]

$$U = \sum_{i,j}\varphi(r_{ij}) + \sum_i F(\rho_i),$$
$$\rho_i = \sum_j \psi(r_{ij}).$$

Here, $\varphi(r)$ is the pair potential of interparticle interaction, and $F(\rho)$ is the embedded function, which effectively takes into account multiparticle correlations via the electron density ρ_i of the ith atom. The supercooled cobalt melt was obtained by rapid cooling of the equilibrium melt (at 2000 K) at a cooling rate of $\gamma = 10^{12}$ K/s [29]. Integration of the equations of motion was carried out according to the Verlet velocity algorithm with a time step of $\tau = 10^{-15}$ s [30]. To bring the system to a state of thermodynamic equilibrium and to calculate the spectral characteristics at each temperature of 1400, 1500, 1600, 1700, 1800, 1900, and 2000 K, the program performed 10^5 and 5×10^6 time steps, respectively.

The simplest way to verify the accuracy of the potential of interparticle interaction to reporoduce of the structural properties of the system is to calculate the radial distribution function of atoms [31]

$$g(r) = \frac{V}{N^2}\left\langle \sum_i \sum_{j\neq i} \delta(r - r_{ij}) \right\rangle,$$

and the statistic structure factor [32, 33]

$$S(k) = 1 + \frac{N}{V}\int [g(r) - 1]\exp[i(\mathbf{k}, \mathbf{r})]\, d\mathbf{r},$$

which can be compared with the experimental X-ray and neutron diffraction data.

Figure 1 shows the radial distribution function $g(r)$ of atoms and the static structure factor $S(k)$ of liquid cobalt at $T = 1873$ K. The simulation results are compared with the experimental X-ray diffraction data [7]. Calculation with the EAM potential [28] yields better agreement with the experimental data compared with the results on the basis of the model potential from [34]: the $S(k)$ components and the full form of the radial distribution function are correctly reproduced[1]. This result is somewhat unexpected, since the poten-

[1] Unfortunately, the authors do not know the experimental data for $S(k)$ of liquid cobalt at other temperatures.

tial, proposed by Pan and Mishin [34], refers to the "new-generation" EAM potentials; therefore, we could quite naturally assume that it reproduces the structural characteristics of the melt more qualitatively.

Calculation of ν using simulation data can be done in several ways. Firstly, it is possible to determine this quantity by the generalized Einstein relation [35, 36]

$$\nu = \frac{m}{k_B TN}\lim_{t\to\infty}\frac{1}{2t}\left\langle\left|\sum_{i=1}^{N}\left[\vartheta_{ix}(t)r_{iy}(t) - \vartheta_{ix}(0)r_{iy}(0)\right]\right|^2\right\rangle.$$

Second, the coefficient ν can be found by the Kubo–Green integral relation [37]

$$\nu = \frac{VS_0}{\rho k_B T}\int_0^\infty S(t)dt,$$

where $S(t)$ is the normalized time correlation function of the stress tensor (the expression for $S(t)$ is presented below) and k_B is the Boltzmann constant.

Lastly, to determine ν, it is possible to use the conclusions of generalized hydrodynamics [37], according to which it is assumed that the generalized kinematic viscosity coefficient $\nu(k,\omega)$ is considered as

$$\nu = \lim_{\omega\to 0}\lim_{k\to 0}\nu(k,\omega).$$

Thus, from the well-known hydrodynamics equation

$$\frac{\partial}{\partial t}C_T(k,t) + \nu k^2 C_T(k,t) = 0$$

we obtain [38, 39]

$$\lim_{\omega\to 0}\nu(k,\omega) = \left(k^2\int_0^\infty C_T(k,t)dt\right)^{-1}, \qquad (1)$$

where $C_T(k,t)$ is the normalized time correlation function of the transverse current [40]:

$$C_T(k,t) = \frac{\left\langle[\mathbf{e}_k, \mathbf{j}^*(k,0)],[\mathbf{e}_k, \mathbf{j}(k,t)]\right\rangle}{\left\langle\left|[\mathbf{e}_k, \mathbf{j}(k,0)]\right|^2\right\rangle}.$$

Here, the scalar and vector products are denoted by parentheses and brackets, respectively; $\mathbf{j}(k,t)$ is the microscopic current expressed by the equation [37, 41]

$$\mathbf{j}(k,t) = \frac{1}{\sqrt{N}}\sum_{l}^{N}\mathbf{v}_l(t)\exp\left[-i\left(\mathbf{k},\mathbf{r}_l(t)\right)\right],$$

where $\mathbf{v}_l(t)$ is the velocity of lth particle at time instant t and $\mathbf{e}_k = \mathbf{k}/|\mathbf{k}|$ is the unit vector codirectional with wave vector $\mathbf{k}$. Conversely, in a long-wavelength limit, the following expression takes place [42]:

$$\lim_{k\to 0}\nu(k,0) = \frac{\nu}{1+\alpha^2 k^2}. \qquad (2)$$

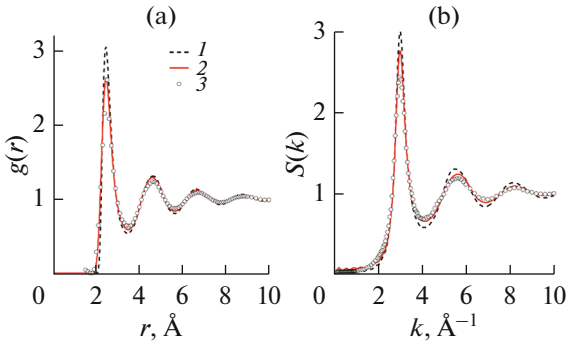

Fig. 1. Radial distribution function of cobalt atoms at T = 1873 K (a) and the static structure factor of the cobalt melt (b): curves–the results of molecular dynamics simulation obtained on the basis of the interatomic interaction model [34] (*1*) and the potential [28] (*2*); (*3*) experimental data on X-ray diffraction [7].

Interpolating the dependence on k for the fixed temperature by means of (2), we can determine the value of the coefficient ν.

THEORETICAL FORMALISM

Let us consider a system consisting of N identical particles of mass m in volume V. We choose the off-diagonal components of the stress tensor [43] as the initial dynamic variable

$$\sigma_{\alpha,\beta} = \frac{1}{V}\left(\sum_{i=1}^{N} m v_{i\alpha}v_{i\beta} - \sum_{i=1}^{N-1}\sum_{j=i+1}^{N} r_{ij\alpha}\frac{\partial U(r_{ij})}{\partial r_{ij\beta}}\right),$$

where $r_{ij} = |\mathbf{r}_i - \mathbf{r}_j|$ is the distance between the particles with indices i and j; $\mathbf{v}_i$ is the vector of particle velocity i; and $U(r_{ij})$ is the potential of interparticle interaction. Indices $\alpha,\beta \in \{x, y, z\}$ denote the projection of values on the corresponding coordinate axis. We determine the time correlation function (TCF) of stress tensor [44, 45]

$$S(t) = \frac{\left\langle\sigma_{\alpha,\beta}(t)\sigma_{\alpha,\beta}(0)\right\rangle}{\left\langle\left|\sigma_{\alpha,\beta}(0)\right|^2\right\rangle},$$

where

$$S_0 = \left\langle\left|\sigma_{\alpha,\beta}(0)\right|^2\right\rangle = \left(\frac{k_B T}{V}\right)^2 + \frac{2\pi n}{15}\frac{k_B T}{V^2}\int_0^\infty r^4 g(r)\left(5B + Ar^2\right)dr,$$

$$B = \frac{1}{r}\frac{\partial U(r)}{\partial r}, \quad A = \frac{1}{r}\frac{\partial B(r)}{\partial r}.$$

The short-time expansion of $S(t)$ can be presented in the form [46]

$$S(t) = 1 - S^{(2)}\frac{t^2}{2!} + S^{(4)}\frac{t^4}{4!} - S^{(6)}\frac{t^6}{6!} + \ldots$$

Here, $S^{(2m)}$ is the even frequency moments[2]

$$S^{(2m)} = \frac{\int \omega^{2m}\tilde{S}(\omega)d\omega}{\int \tilde{S}(\omega)d\omega}, \quad m = 1, 2, \ldots \tag{3}$$

of the spectral density of TCF of the stress tensor [20]

$$\tilde{S}(\omega) = \frac{S(t=0)}{2\pi}\mathrm{Re}\int_{-\infty}^{\infty}\exp(i\omega t)S(t)dt.$$

Conversely, the spectral density of the TCF of the stress tensor $\tilde{S}(\omega)$ can be represented in the form [48]

$$\tilde{S}(\omega) = \frac{S(t=0)}{\pi}\mathrm{Re}\left\{\frac{1}{-i\omega + \Delta_1\tilde{M}_1(\omega)}\right\},$$

where $\tilde{M}_1(\omega)$ is the spectral density of so-called first-order memory function, which is connected with the high-order memory functions $\tilde{M}_n(\omega)$ at $n > 1$ by the recurrence relation[3]

$$\tilde{M}_n(\omega) = \left(-i\omega + \Delta_{n+1}\tilde{M}_{n+1}(\omega)\right)^{-1},$$

and Δ_n are the frequency parameters, which are expressed by the spectral moments $S^{(2m)}$, $n, m = 1, 2, \ldots$:

$$\Delta_1 = S^{(2)},$$
$$\Delta_2 = \frac{S^{(4)}}{S^{(2)}} - S^{(2)},$$
$$\Delta_3 = \frac{S^{(6)}S^{(2)} - S^{(4)^2}}{S^{(4)}S^{(2)} - S^{(2)^3}},$$
$$\ldots.$$

In accordance with the Kubo–Green formula for kinematic viscosity ν, we have [20]

$$\nu = \frac{VS_0}{\rho k_B T}\int_0^{\infty} S(t)dt = \frac{VS_0}{\rho k_B T}\tilde{S}(\omega = 0). \tag{4}$$

As shown in [51, 52], the condition $\tilde{M}_2(\omega) = \tilde{M}_1(\omega)$ is realized for transport processes in single-component liquids, which allows us to find an expression for the spectral density

$$\tilde{S}(\omega) = \frac{1}{\pi}\frac{2\Delta_1\Delta_2\sqrt{4\Delta_2 - \omega^2}}{\Delta_1^2\left(4\Delta_2 - \omega^2\right) + \omega^2\left(2\Delta_2 - \Delta_1\right)^2}. \tag{5}$$

From this, we obtain a simple expression for the kinematic viscosity

$$\nu = \frac{VS_0}{\pi\rho k_B T}\frac{\sqrt{\Delta_2}}{\Delta_1}. \tag{6}$$

Here, the frequency parameter Δ_1 is determined by an integral expression containing $U(\mathbf{r})$ and the radial distribution functions of two and three particles, $g(\mathbf{r})$ and $g_3(\mathbf{r}_1, \mathbf{r}_2)$, respectively. For numerical estimation of parameter Δ_2, it is also necessary to know the distribution function of four particles $g_4(\mathbf{r}_1, \mathbf{r}_2, \mathbf{r}_3)$ (see expressions (5) and (6) in [47]).

RESULTS

Figure 2 shows a comparison of the results of theoretical calculations for the spectral density $\tilde{S}(\omega)$ of the cobalt melt by Eq. (5) with molecular dynamics simulation data. The frequency moments of the spectral density of the stress tensor TCF $\tilde{S}(\omega)$ used in the calculations are presented in Table 1. The values of the moment $S^{(0)}$ were determined from the condition for normalizing the TCF of the stress tensor $S(t = 0) = 1$, the frequency moment $S^{(2)}$ was calculated by numerical integration of the simulation spectra in accordance with the relation (3), and the fourth moment $S^{(4)}$ was

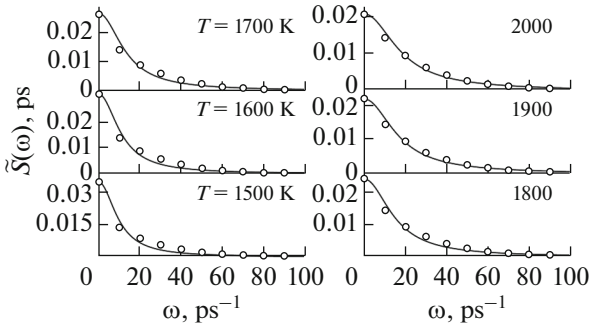

Fig. 2. Spectral density of the time correlation function of the stress tensor $\tilde{S}(\omega)$ of the cobalt melt at various temperatures: curves stand for the results of theoretical calculations according to Eq. (5), dots—molecular dynamics simulation data.

Table 1. Frequency moments $S^{(2m)}$ of the spectral density TCF of the stress tensor (5) and the fitting parameters to the expression (2) for the cobalt melt at $p = 1.5$ bar

T, K	S_0, 10^{16} Pa^2	$S^{(2)}$, 10^{26} s^{-2}	$S^{(4)}$, 10^{54} s^{-4}	α, Å
1400	2.107	6.455	4.858	0.54
1500	2.162	6.804	4.251	0.54
1600	2.203	7.120	3.953	0.54
1700	2.228	7.479	3.504	0.54
1800	2.248	7.876	3.422	0.55
1900	2.260	8.162	3.263	0.58
2000	2.274	8.484	3.228	0.60

[2] The microscopic expressions for the frequency moments of $S^{(2)}$ and $S^{(4)}$ are presented in [47].

[3] We note that in the time domain this relation can be represented as an infinite chain of integro-differential Zwanzig–Mori kinetic equations [49, 50].

found by comparing the theory with the simulation results. The theoretical curves correctly reproduce all of the features of the $\tilde{S}(\omega)$ spectra at all of the considered temperatures, which indicates indirectly the correctness of the theoretical model (6). At the same time, comparison with experimental data (for example, inelastic scattering of neutrons or X-rays) is required in order to unambiguously conclude that the EAM potential from [28] is able to reproduce correctly the microscopic dynamics of the cobalt melt in the considered temperature range. At the moment, such experimental data are not available.

Figure 3 shows the simulation results for the wave number dependence of the kinematic viscosity at various temperatures. The values ν were directly determined by the interpolation of these curves into the region of small values of k. Table 1 presents the parameters obtained as a result of fitting expression (2) to $\nu(k,0)$ from the simulation. Figure 4 shows the temperature dependence of the kinematic viscosity for the cobalt melt at the pressure $p = 1.5$ bar. The results of theoretical calculations (6) for the temperature dependence of the kinematic viscosity of the cobalt melt are in good agreement with both the molecular dynamics simulation results and with the experimental data. We note that the obtained results and experimental results have minor discrepancies as compared to the experimental data of previous measurements [22, 53].

As is known, for equilibrium liquids, the temperature dependence of the viscosity should be determined by the Arrhenius thermal activation law

$$\nu(T) = \nu_0 \exp\left(\frac{E}{k_B T}\right), \qquad (7)$$

where ν_0 is the preexponential factor corresponding to the formal value of viscosity at $T \to \infty$ and E is the height (energy) of activation barrier of viscosity process. The dependence of viscosity $\nu(T)$ on the temperature is presented in Fig. 4 in a logarithmic scale. Fitting by Eq. (7) was performed with the parameters $\nu_0^{MD} = (5.4 \pm 0.05) \times 10^{-8}$ m^2/s ($\nu_0^{Exp} = (6.3 \pm 0.1) \times 10^{-8}$ m^2/s) and $E^{MD} = (5.4 \pm 0.02) \times 10^{-20}$ J ($E^{Exp} = (5.35 \pm 0.05) \times 10^{-20}$ J) for simulation and experiment, respectively. It can be seen that the results of the present experiment and the simulation for the temperature dependence of the kinematic viscosity are reproduced well by the Arrhenius relation (7). It should be noted that the experimental values at $T < 1631$ K begin to deviate insignificantly from this dependence. At the same time, the experimental data [53] are closer to the results of simulation and have a smaller scattering in comparison with the experimental results of this work. The experimental values of the viscosity from [22] cover the high-temperature region of 1800–2100 K. Although these data approximate the results of numerical calculations at high temperatures,

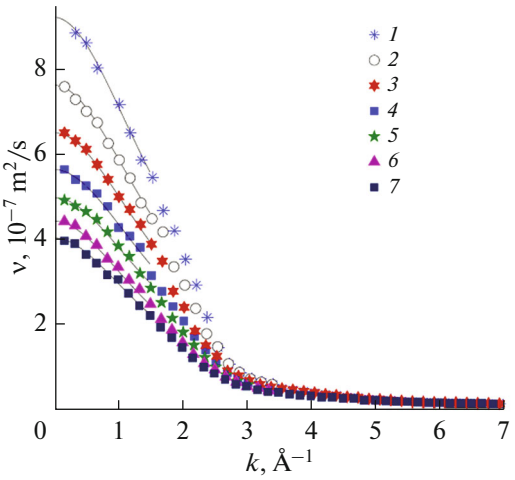

Fig. 3. Wave number dependences of the kinematic viscosity of the cobalt melt at $p = 1.5$ bar and various temperatures, obtained on the basis of simulation data: (*1*) $T =$ 1400 K, (*2*) 1500, (*3*) 1600, (*4*) 1700, (*5*) 1800, (*6*) 1900, (*7*) 2000; solid lines show the results of the fitting procedure with (2).

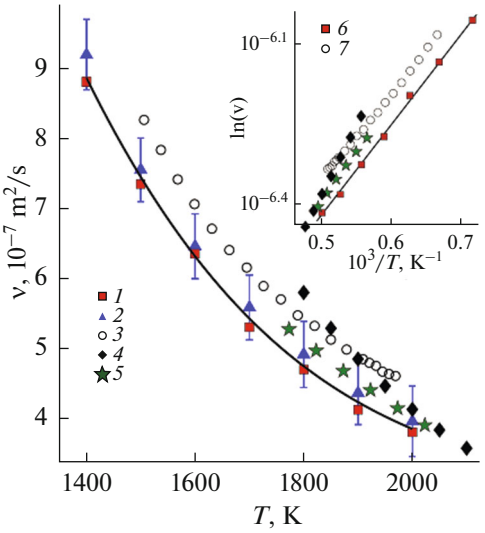

Fig. 4. The temperature dependence of the kinematic viscosity of the cobalt melt at $p = 1.5$ bar: (*1*, *2*) results of molecular dynamics simulation calculated with the Kubo–Green relation for $S(t)$ (formula (4)) and in the framework of generalized hydrodynamics with $C_T(k, t)$ (Eqs. (1) and (2)), respectively; (*3*) experimental results; solid line—the results of theoretical calculations performed according to (6); (*4*) and (*5*) experimental data from [22] and [53], respectively; on the inset—the dependence in a logarithmic scale: (*6*, *7*) the results of simulation and experimental results, respectively; solid line—results of fitting with (7).

the character of the temperature dependence of $\nu(T)$ in accordance with these experimental data differs both from other experiments and simulation results. Thus, we can estimate the values of ν_0 and E, and thus obtain $\bar{\nu}_0 = (5.8 \pm 0.1) \times 10^{-8}$ m^2/s and $\bar{E} = (5.38 \pm 0.02) \times 10^{-20}$ J.

CONCLUSIONS

The viscosity properties of cobalt melt in a temperature range of 1400–2000 K at $p = 1.5$ bar were investigated experimentally by the torsional vibration method and numerically by molecular dynamics simulation with the EAM potential of interparticle interaction [28]. To verify the accuracy of the considered EAM potential to reproduce the particle dynamics in the cobalt melt, the structural characteristics of the system (the radial distribution function and the static structure factor) were calculated. They show good agreement with the experimental data on X-ray diffraction [7]. Calculation of the kinematic viscosity on the basis of the results of molecular dynamics simulation was carried out in two ways: with the Kubo–Green integral relation for $S(t)$ and within the framework of generalized hydrodynamics with TCF of the transverse current $C_T(k, t)$. It is shown that both the methods lead to similar temperature dependences of the kinematic viscosity, which are in good agreement with the experimental results of viscosimetry.

Within the formalism of memory functions and the self-consistent approach [51, 52], expressions were obtained for the spectral density of the stress tensor time correlation function $\tilde{S}(\omega)$ and kinematic viscosity, which are determined from the frequency parameters Δ_1 and Δ_2. The results of theoretical calculations of the temperature dependence of the viscosity $\nu(T)$ of the cobalt melt are in good agreement with both the results of molecular dynamics simulations and with the experimental data.

ACKNOWLEDGMENTS

Large-scale molecular dynamics calculations were performed on the computing cluster of the Kazan Federal University and the supercomputer of the Interdepartmental Supercomputer Center of the Russian Academy of Sciences. This work was supported by the Ministry of Eduction and Science of the Russian Federation via Kazan State University in teh framework of the task 3.2166.2017/4.6 and by the grant from the President of the Russian Federation MD-5792.2016.2.

REFERENCES

1. Sarkisov, G.N., *Phys.—Usp.*, 2002, vol. 45, no. 6, p. 597.
2. Angell, C.A., Ngai, K.L., McKenna, G.B., McMillan, P.F., and Martin, S.W., *J. Appl. Phys.*, 2000, vol. 88, no. 6, p. 3113.
3. Götze, W., *Complex Dynamics of Glass-Forming Liquids*, Oxford: Oxford Univ. Press, 2009.
4. Trachenko, K. and Brazhkin, V.V., *Rep. Prog. Phys.*, 2016, vol. 79, no. 1, 016502.
5. Angell, C.A., *Science*, 1995, vol. 267, no. 5206, p. 1924.
6. Inoue, A., *Acta Mater.*, 2000, vol. 48, no. 1, p. 279.
7. Waseda, Y., *The Structure of Non-Crystalline Materials: Liquids and Amorphous Solids*, New York: McGraw-Hill, 1980.
8. Iida, T. and Guthrie, R.I.L., *The Physical Properties of Liquid Metals*, Oxford: Clarendon, 1993.
9. Khusnutdinoff, R.M., Mokshin, A.V., and Khadeev, I.I., *J. Surf. Invest.: X-ray, Synchrotron Neutron Tech.*, 2014, vol. 8, no. 1, p. 84.
10. Khusnutdinoff, R.M., Mokshin, A.V., Klumov, B.A., Ryltsev, R.E., and Chtchelkachev, N.M., *JETP*, 2016, vol. 123, no. 4, p. 735.
11. Nishiyama, N. and Inoue, A., *Acta Mater.*, 1999, vol. 47, no. 5, p. 1487.
12. Khusnutdinoff, R.M. and Mokshin, A.V., *Bull. Russ. Acad. Sci.: Phys.*, 2010, vol. 74, no. 5, p. 640.
13. Kuiying, C., Hongbo, L., Xiaoping, L., Qiyong, H., and Zhuangqi, H., *J. Phys.: Condens. Matter*, 1995, vol. 7, no. 12, p. 2379.
14. Chen, H.C. and Lai, S.K., *Phys. Rev. E: Stat. Phys., Plasmas, Fluids, Relat. Interdiscip. Top.*, 1997, vol. 56, no. 4, p. 4381.
15. Cherne, F.J., Baskes, M.I., Schwarz, R.B., Srinivasan, S.G., and Klein, W., *Model. Simul. Mater. Sci. Eng.*, 2004, vol. 12, no. 6, p. 1063.
16. Kim, T.H. and Kelton, K.F., *J. Chem. Phys.*, 2007, vol. 126, no. 5, 054513.
17. Cao, Q.-L., Huang, D.-H., Yang, J.-S., Wan, M.-J., and Wang, F.-H., *Phys. B (Amsterdam, Neth.)*, 2014, vol. 450, p. 136.
18. Evteev, A.V., Kosilov, A.T., Levchenko, E.V., and Logachev, O.B., *Phys. Solid State*, 2006, vol. 48, no. 5, p. 815.
19. Mokshin, A.V., Khusnutdinoff, R.M., Novikov, A.G., Blagoveshchenskii, N.M., and Puchkov, A.V., *JETP*, 2015, vol. 121, no. 5, p. 828.
20. March, N.H., *Liquid Metals: Concepts and Theory*, Cambridge: Cambridge University Press, 1990.
21. Scopigno, T., Ruocco, G., and Sette, F., *Rev. Mod. Phys.*, 2005, vol. 77, no. 3, p. 881.
22. Assael, M.J., Armyra, I.J., Brillo, J., Stankus, S.V., Wu, J., and Wakeham, W.A., *J. Phys. Chem. Ref. Data*, 2012, vol. 41, no. 3, 033101.
23. Shvidkovskii, E.G., *Nekotorye voprosy vyazkosti rasplavlennykh metallov* (Some Issues of the Viscosity of Molten Metals), Moscow: Gostekhizdat, 1955.
24. Bel'tyukov, A.L. and Lad'yanov, V.I., *Instrum. Exp. Tech.*, 2008, vol. 51, no. 2, p. 304.
25. Goncharov, O.Yu., Olyanina, N.V., Bel'tyukov, A.L., and Lad'yanov, V.I., *Russ. J. Phys. Chem. A*, 2015, vol. 89, no. 5, p. 842.
26. Samsonov, G.V., Borisova, A.L., Zhidkova, T.G., et al., *Fiziko-khimicheskie svoistva okislov* (Physical and Chemical Properties of Oxides), Moscow: Metallurgiya, 1978.
27. Bel'tyukov, A.L., Lad'yanov, V.I., and Shishmarin, A.I., *High Temp.*, 2014, vol. 52, no. 2, p. 185.
28. Passianot, R. and Savino, E.J., *Phys. Rev. B: Condens. Matter Mater. Phys.*, 1992, vol. 45, no. 22, p. 12704.
29. Khusnutdinov, R.M., Mokshin, A.V., and Yul'met'ev, R.M., *JETP*, 2009, vol. 108, no. 3, p. 417.
30. Allen, M.P. and Tildesley, D.J., *Computer Simulation of Liquids*, Oxford: Clarendon, 1987.
31. Khusnutdinoff, R.M. and Mokshin, A.V., *J. Non-Cryst. Solids*, 2011, vol. 357, no. 7, p. 1677.
32. Frenkel', Ya.I., *Kineticheskaya teoriya zhidkostei* (Kinetic Theory of Liquids), Leningrad: Nauka, 1975.

33. Khusnutdinoff, R.M. and Mokshin, A.V., *Phys. A (Amsterdam, Neth.)*, 2012, vol. 391, no. 9, p. 2842.
34. Pun, G.P.P. and Mishin, Y., *Phys. Rev. B: Condens. Matter Mater. Phys.*, 2012, vol. 86, no. 13, 134116.
35. Einstein, A., *Investigation on the Theory of the Brownian Movement*, New York: Dover, 1926.
36. Copley, J.R.D. and Lovesey, S.W., *Rep. Prog. Phys.*, 1975, vol. 38, no. 4, p. 461.
37. Hansen, J.P. and McDonald, I.R., *Theory of Simple Liquids*, New York: Academic, 2006.
38. Gaskell, T., Balucani, U., Gori, M., and Vallauri, R., *Phys. Scr.*, 1987, vol. 35, no. 1, p. 37.
39. Khusnutdinoff, R.M., Mokshin, A.V., Menshikova, S.G., Beltyukov, A.L., and Ladyanov, V.I., *JETP*, 2016, vol. 122, no. 5, p. 859.
40. Montfrooij, W. and de Schepper, I., *Excitations in Simple Liquids, Liquid Metals, and Superfluids*, New York: Oxford University Press, 2010.
41. Khusnutdinoff, R.M. and Mokshin, A.V., *JETP Lett.*, 2014, vol. 100, no. 1, p. 39.
42. Alley, W.E. and Alder, B.J., *Phys. Rev. A: At., Mol., Opt. Phys.*, 1983, vol. 27, no. 6, p. 3158.
43. Boon, J.P. and Yip, S., *Molecular Hydrodynamics*, New York: McGraw-Hill, 1980.
44. Balucani, U. and Zoppi, M., *Dynamics of the Liquid State*, Oxford: Clarendon, 1994.
45. Forster, D., Martin, P.C., and Yip, S., *Phys. Rev.*, 1968, vol. 170, no. 1, p. 155.
46. Mokshin, A.V., Chvanova, A.V., and Khusnutdinoff, R.M., *Theor. Math. Phys.*, 2012, vol. 171, no. 1, p. 541.
47. Tankeshwar, K., Pathak, K.N., and Ranganathan, S., *J. Phys. C: Solid State Phys.*, 1988, vol. 21, no. 19, p. 3607.
48. Mokshin, A.V., Yulmetyev, R.M., Khusnutdinov, R.M., and Hänggi, P., *JETP*, 2006, vol. 103, no. 6, p. 841.
49. Zwanzig, R., *Phys. Rev.*, 1961, vol. 124, no. 4, p. 983.
50. Mori, H., *Prog. Theor. Phys.*, 1965, vol. 33, no. 3, p. 423.
51. Yulmetyev, R.M., Mokshin, A.V., and Hänggi, P., *Phys. Rev. E: Stat., Nonlinear, Soft Matter Phys.*, 2003, vol. 68, no. 5, 051201.
52. Mokshin, A.V., Yulmetyev, R.M., and Hänggi, P., *New J. Phys.*, 2005, vol. 7, p. 9.
53. *CRC Handbook of Chemistry and Physics*, Lide, D.R., Ed., Boca Raton: CRC, 2008–2009, 89th ed.

Translated by A. Bannov